ADVANCED MATERIALS TECHNOLOGIES

Supporting Information

for *Adv. Mater. Technol.,* DOI: 10.1002/admt.202200387

Superrepellent Doubly Reentrant Geometry Promotes Antibiofouling and Prevention of Coronavirus Contamination

*Meng-Shiue Lee, Yueh Chien, Pai-Chi Teng, Xuan-Yang Huang, Yi-Ying Lin, Ting-Yi Lin, Shih-Jie Chou, Chian-Shiu Chien, Yu-Jer Hsiao, Yi-Ping Yang, Wensyang Hsu, and Shih-Hwa Chiou**

Supporting Information

Superrepellent doubly reentrant geometry promotes antibiofouling and prevention of coronavirus contamination

Detailed deduction of the ratio of the real contact area (*i.e.*, liquid-solid area) to the (liquid volume)$^{2/3}$ vs. intrinsic contact angle (*i.e.*, Young's angle) for Cassie-droplets:

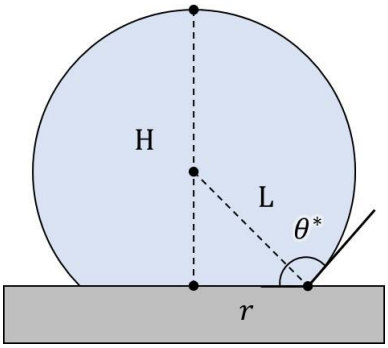

When the Cassie-droplet volume is tiny, we assume the liquid is a sphere cut by a plane (as in the figure above) due to the capillary action. We can get $\boldsymbol{L = \frac{r}{\sin\theta^*}}$ and $\boldsymbol{H = r\tan\frac{\theta^*}{2}}$.

The droplet volume $\boldsymbol{V = \frac{\pi}{3}H^2(3L - H)}$. After replacing L and H, we can get

$$\boldsymbol{V = \frac{\pi}{3}r^3\tan^2\frac{\theta^*}{2}\left(\frac{3}{\sin\theta^*} - \tan\frac{\theta^*}{2}\right)}$$

The contact region (in the macroscopic view) $\boldsymbol{R_C = \pi r^2}$. By replacing r with V, we can get

$$\boldsymbol{R_C = \pi\left(\frac{3V}{\pi\tan^2\frac{\theta^*}{2}\left(\frac{3}{\sin\theta^*} - \tan\frac{\theta^*}{2}\right)}\right)^{\frac{2}{3}}}$$

$$\boldsymbol{by\ \sin\theta^* = \frac{2\tan\frac{\theta^*}{2}}{1 + \tan^2\frac{\theta^*}{2}}}$$

$$\boldsymbol{R_C = \pi\left(\frac{3V}{\pi\frac{\tan\frac{\theta^*}{2}\left(3 + \tan^2\frac{\theta^*}{2}\right)}{2}}\right)^{\frac{2}{3}}}$$

$$by\ \tan\frac{\theta^*}{2} = \left(\frac{1-\cos\theta^*}{1+\cos\theta^*}\right)^{\frac{1}{2}}$$

$$R_C = \pi\left(\frac{3V}{\pi}\right)^{\frac{2}{3}}(1+\cos\theta^*)\left(\frac{1}{2+3(1+\cos\theta^*)-(1+\cos\theta^*)^3}\right)^{\frac{1}{3}}$$

$$Cassie\ equation\text{: } \cos\theta^* = f_s\cos\theta_Y - (1-f_s) \rightarrow (\cos\theta^*+1) = \left(f_s(\cos\theta_Y+1)\right)$$

$$R_C = (V)^{\frac{2}{3}}\left(3\pi^{\frac{1}{2}}\right)^{\frac{2}{3}}\left(f_s(\cos\theta_Y+1)\right)\left(\frac{1}{2+3\left(f_s(\cos\theta_Y+1)\right)-\left(f_s(\cos\theta_Y+1)\right)^3}\right)^{\frac{1}{3}}$$

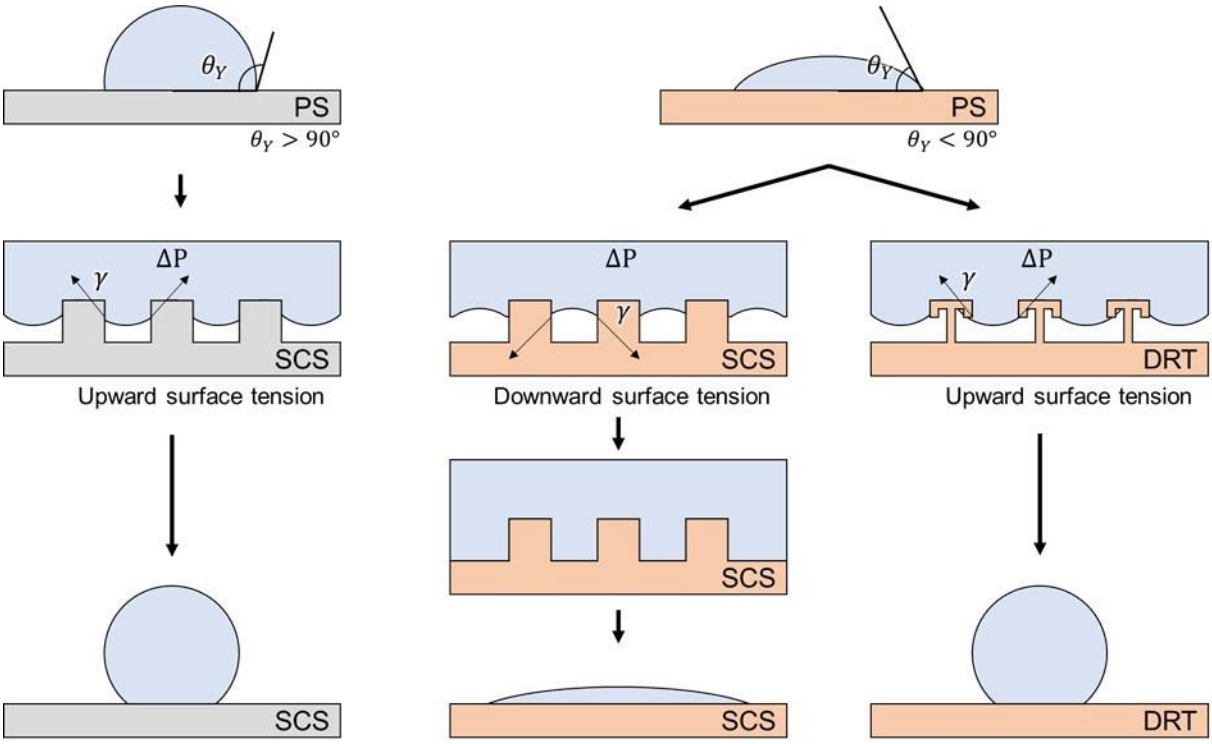

Supplementary Figure S1. Liquid suspension on the SCS and DRT surface. The liquid suspension is achieved through the upward surface tension. Under the condition of an intrinsic contact angle of $< 90°$, the liquid immerses the structure of SCS but is suspended on the DRT surface.

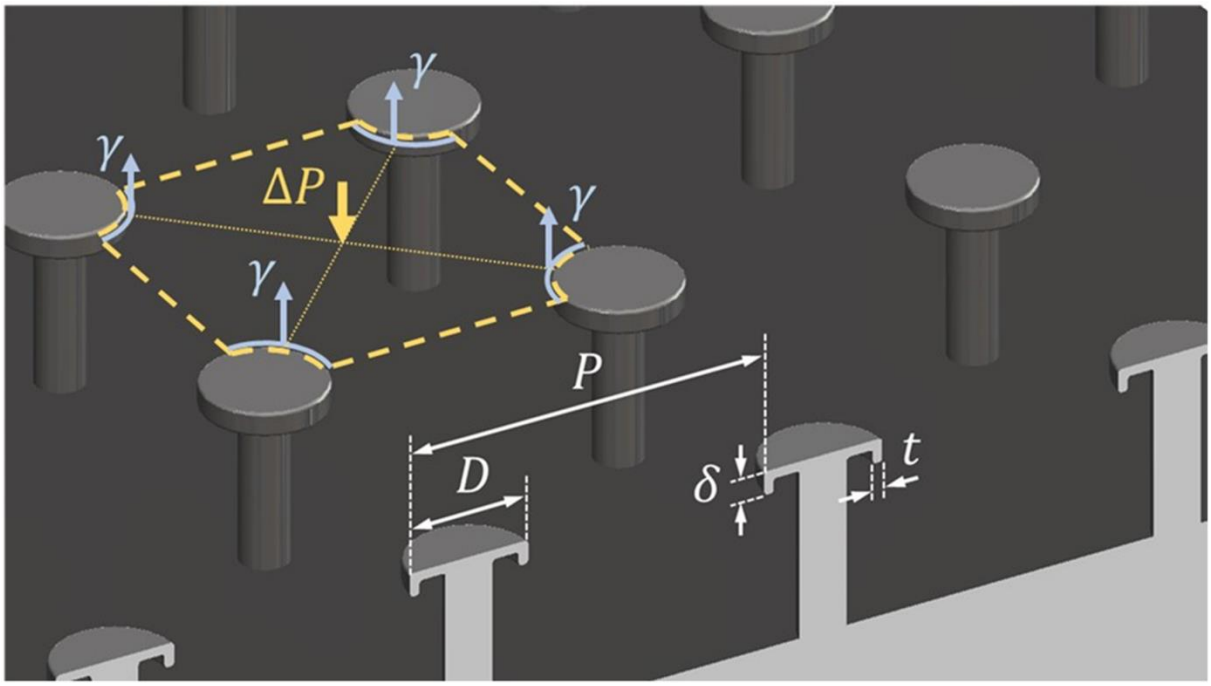

Supplementary Figure S2. Key geometric parameters of the DRT surface. D is the post top diameter, P is the center-to-center distance (*i.e.*, pitch) between the adjacent posts, and d and t are the length and thickness, respectively, of the overhang. The fabricated DRT surface is a square array of circular posts with D ~10 μm, P ~ 50 μm, δ ~ 1.5 μm, and t ~ 300 nm. The height of the columns is ~ 25 μm.

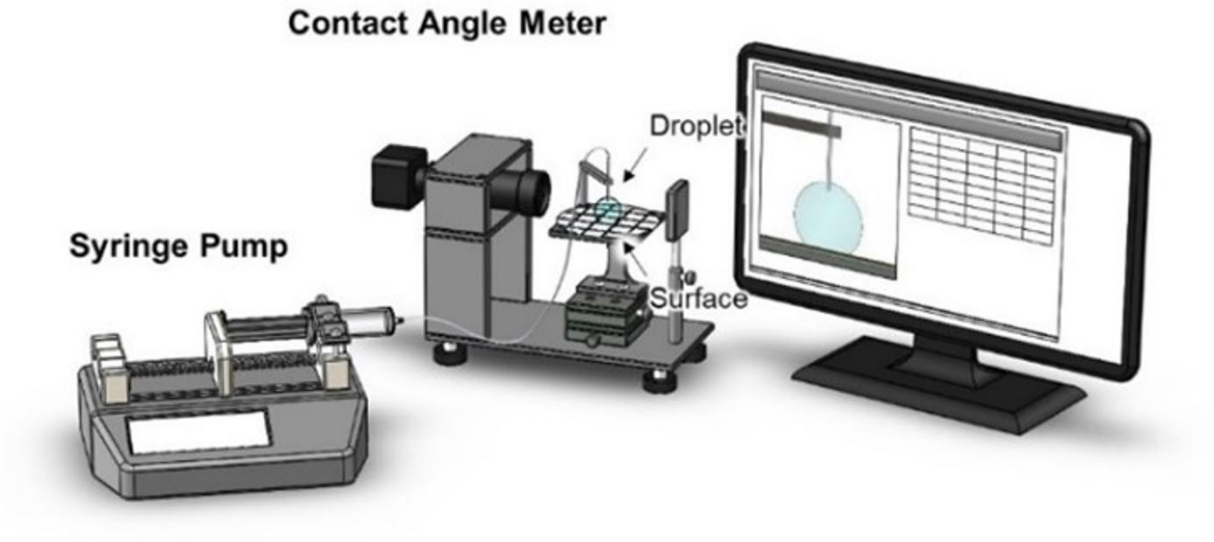

Supplementary Figure S3. The setup of contact angle measurement.

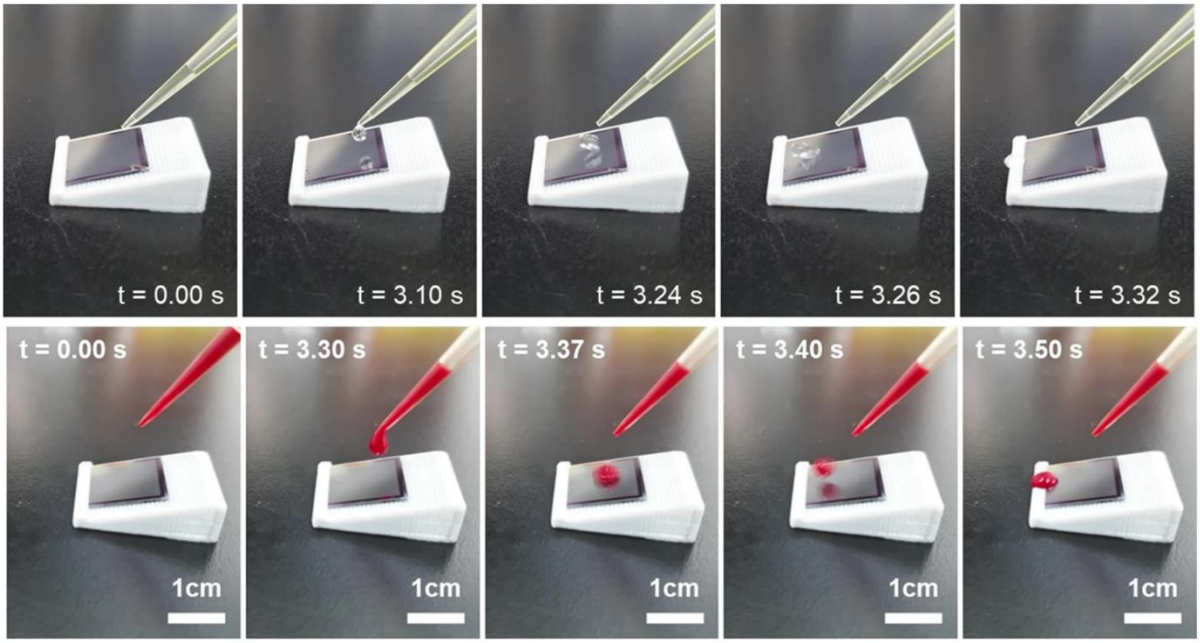

Supplementary Figure S4. The antibiofouling performance of the SiO_2-DRT surface at a tilted angle. The droplet of ddH_2O (upper row) and blood (lower row) quickly rolled off the surface within 3.5 seconds.

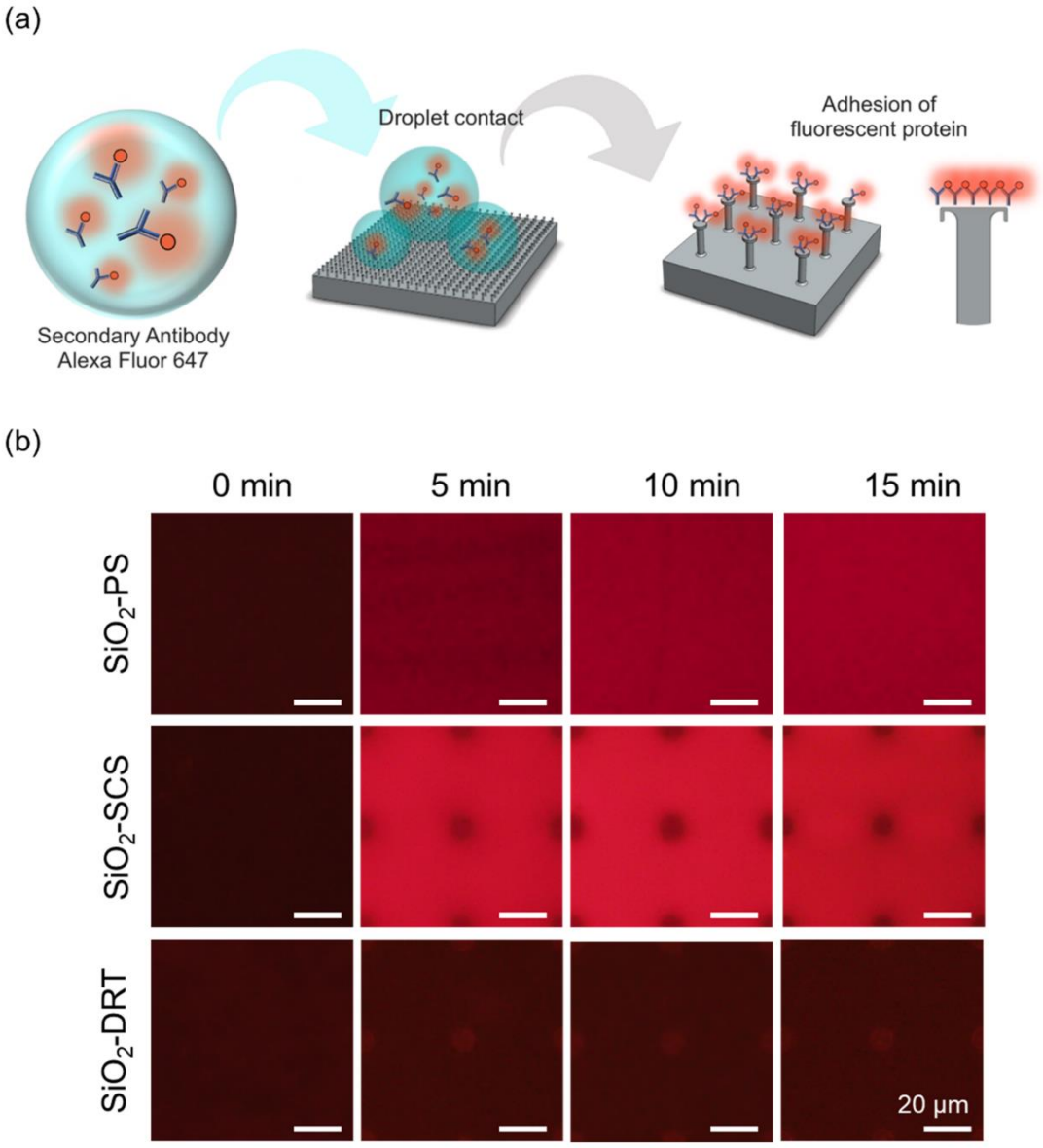

Supplementary Figure S5. Antifouling effect of different surfaces against protein fouling. **(a)** The test for antibiofouling of protein on surfaces. The protein solution with fluorescence reporter was placed on the surfaces for a different duration. Then, we measured the fluorescence intensity of adherent proteins on the surfaces and defined it as protein fouling. (b) The fluorescence microscopy imaging shows the protein biofouling on different surfaces.

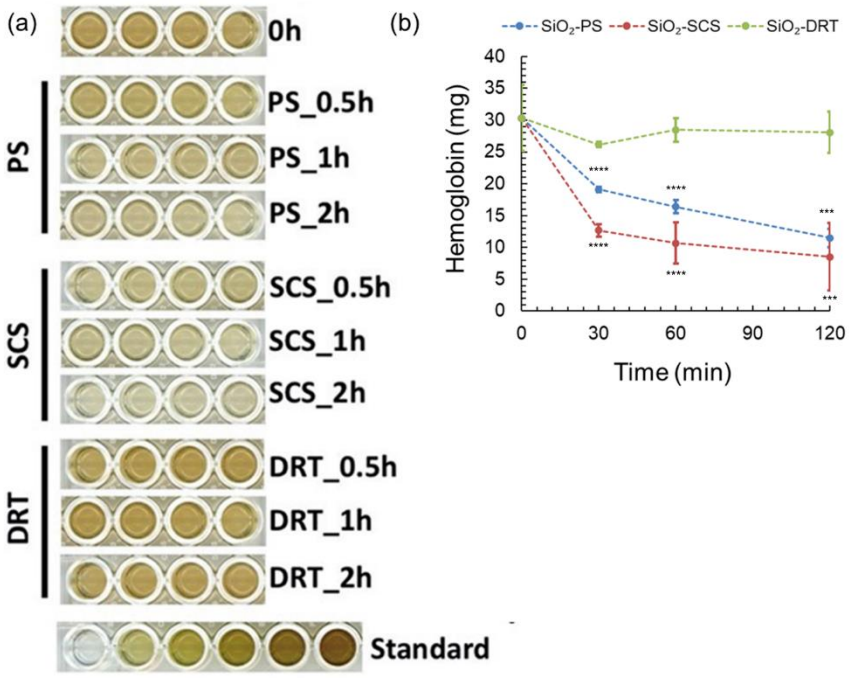

Supplementary Figure S6. Antifouling effect of different structured surfaces against blood. (a) A representative colorimetric analysis of hemoglobin in the droplets recycled from different surfaces. **(b)** Quantification of hemoglobin in the recycled blood droplet from different surfaces. Data shown are mean ± SD. Denotation: ns, $p > 0.05$; * $p \leq 0.05$; ** $p \leq 0.01$; *** $p \leq 0.001$; **** $p \leq 0.0001$ vs. SiO_2-DRT alone.

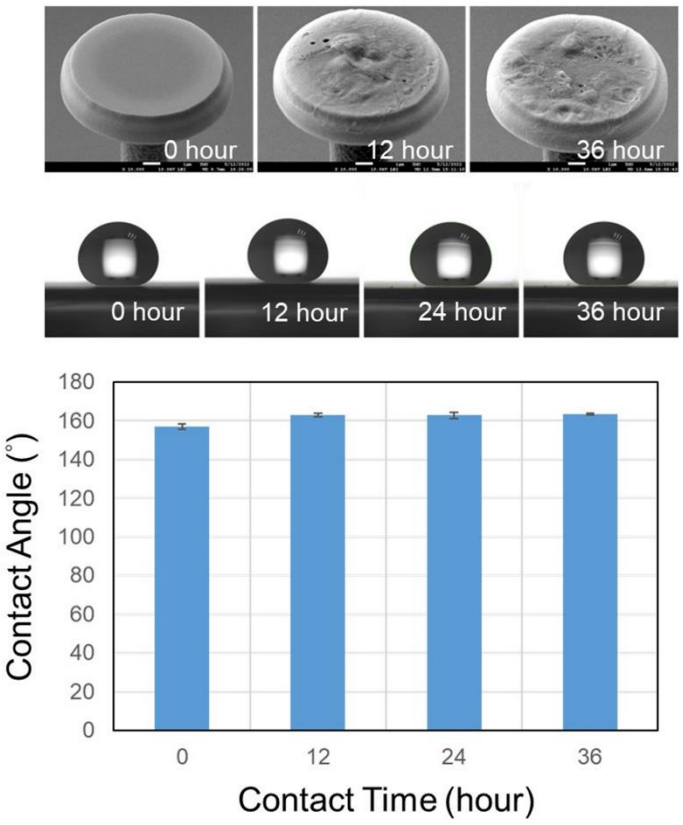

Supplementary Figure S7. Prolonged contact of blood on the SiO_2-DRT surface. The SEM imaging demonstrated residual matters on the surface but did not alter the DRT geometry. The contact angles were all >150° after 0-, 12-, 24-, and 36-hour contact.

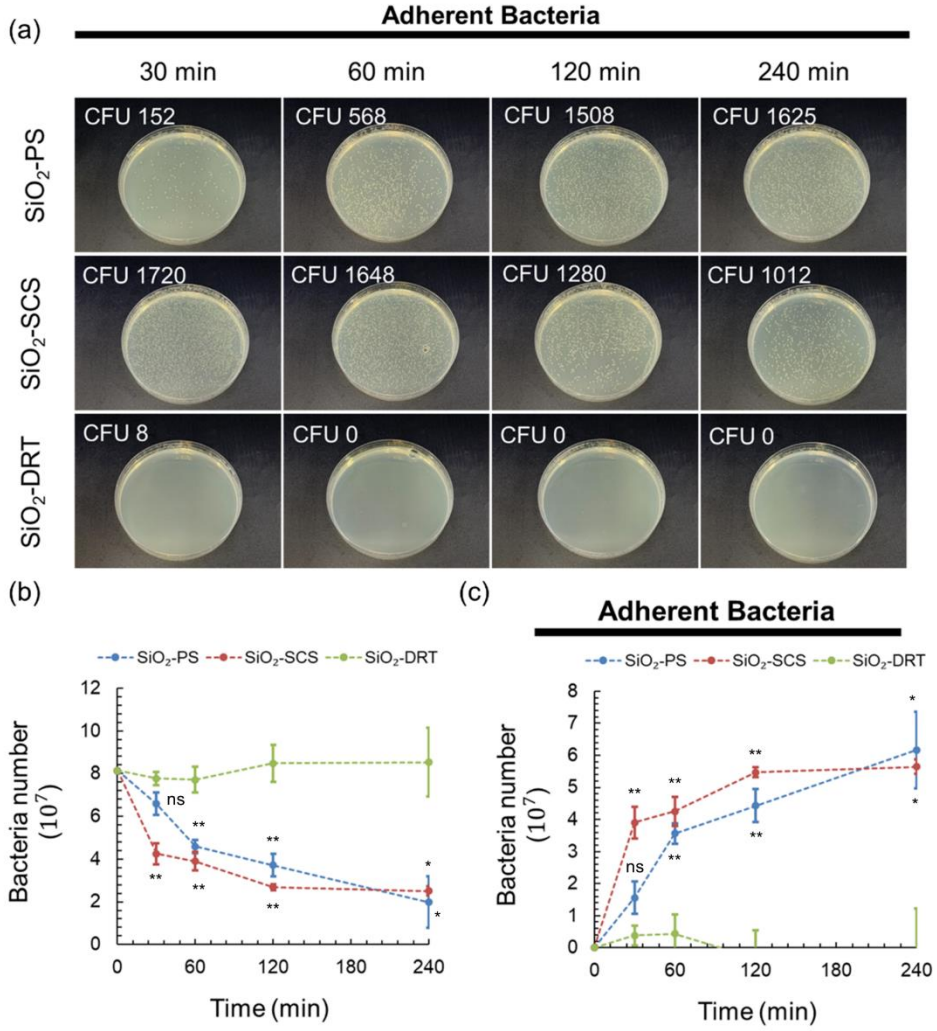

Supplementary Figure S8. Antifouling effect of different surfaces against bacteria. (a) Comparison of colony formation in the plates spread by the adherent bacteria recycled from different surfaces. Adherent bacteria were detached by trypsinization. **(b)** Determination of bacteria concentration on the SiO_2-PS, SiO_2-SCS, and SiO_2-DRT surface using a spectrophotometric method of 600 nm wavelength. **(c)** The amount of the adherent bacteria was calculated and estimated by subtracting droplet bacteria from the loading bacteria. Data shown are mean ± SD. Denotation: ns, $p > 0.05$; * $p \leq 0.05$; ** $p \leq 0.01$; *** $p \leq 0.001$; **** $p \leq 0.0001$ vs. SiO_2-DRT alone.

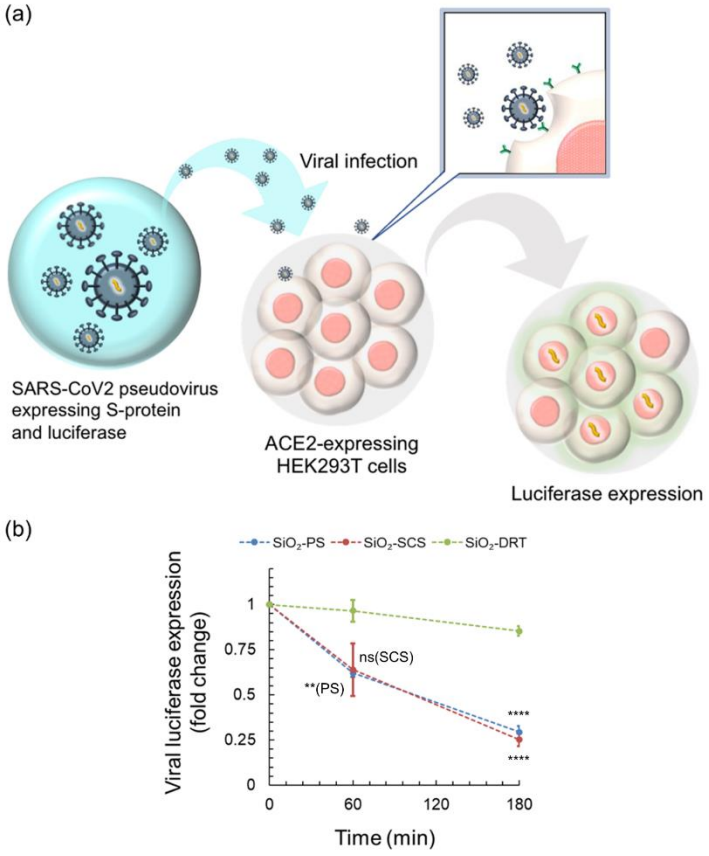

Supplementary Figure S9. Antifouling effect of different surfaces against viruses. (a) After being placed on the surfaces, the virus droplets were recycled and subjected to infecting ACE2-overexpressing HEK293T cells. The luciferase expression was evaluated using qPCR. **(b)** Comparison of viral replicative activity from the virus droplets on different surfaces. Data shown are mean ± SD. Denotation: ns, $p > 0.05$; * $p \leq 0.05$; ** $p \leq 0.01$; *** $p \leq 0.001$; **** $p \leq 0.0001$ vs. SiO_2-DRT alone.

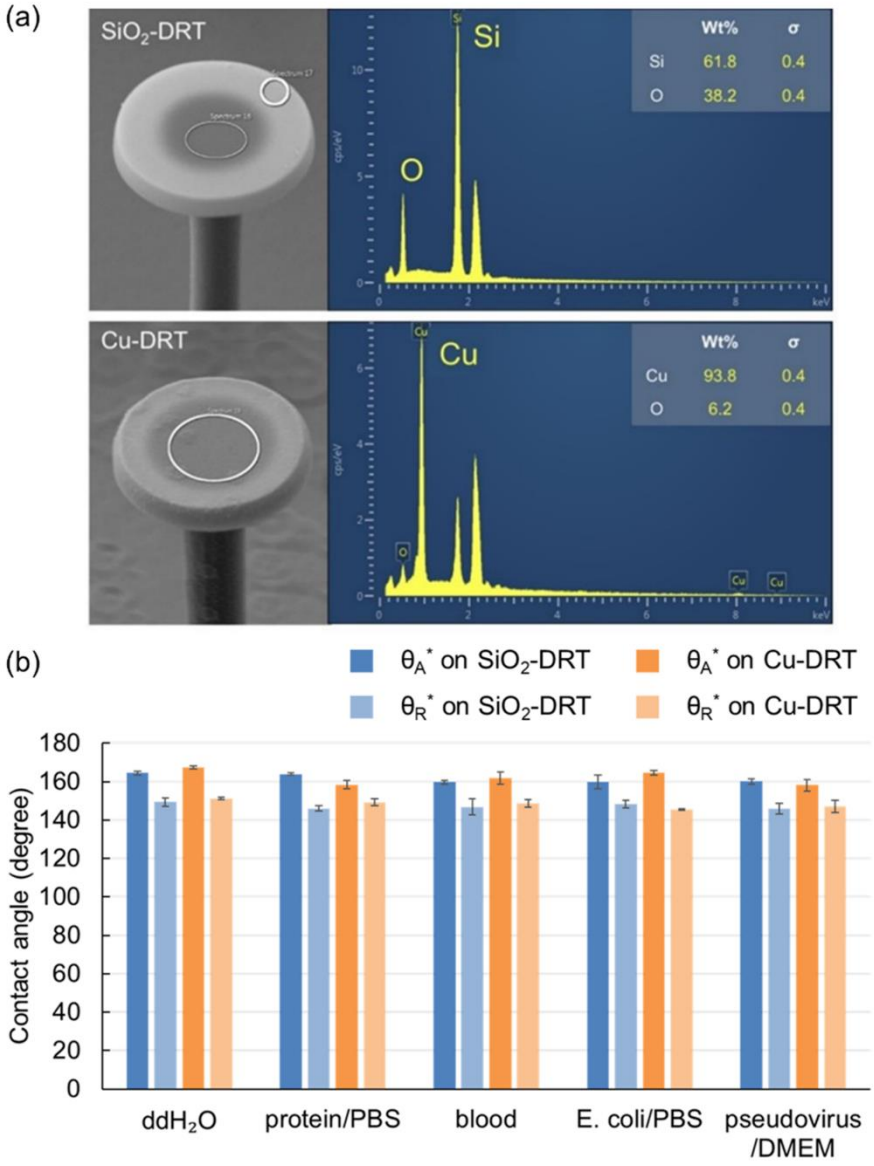

Supplementary Figure S10. (a) The elemental analysis of SiO_2-DRT and Cu-DRT. **(b)** The dynamic contact angle measurement of DRT surfaces. For all test bioliquids, all advancing angles are larger than 150°, and all receding angles are around 150°.

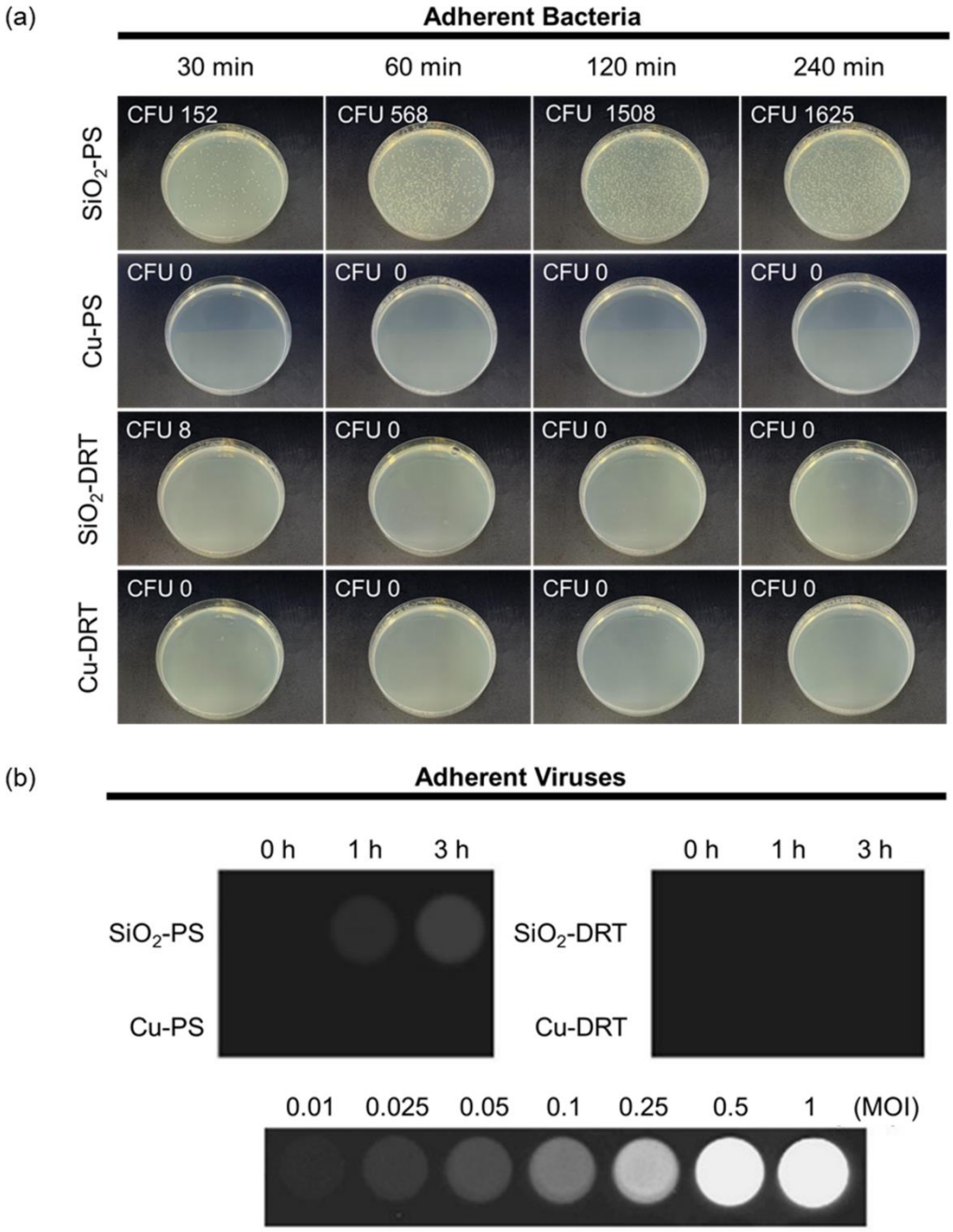

Supplementary Figure S11. (a) Comparison of colony formation in the plates spread by the adherent bacteria recycled from different surfaces with or without copper coating. Adherent bacteria were detached by trypsinization. The bacterial fouling with or without the copper coating was assessed using the CFU method. (b) Adherent viruses were detached by trypsinization. Luciferase reporter assay showed the virus replicative activity from the virus-containing droplets or adhesive viruses on surfaces with or without copper coating.

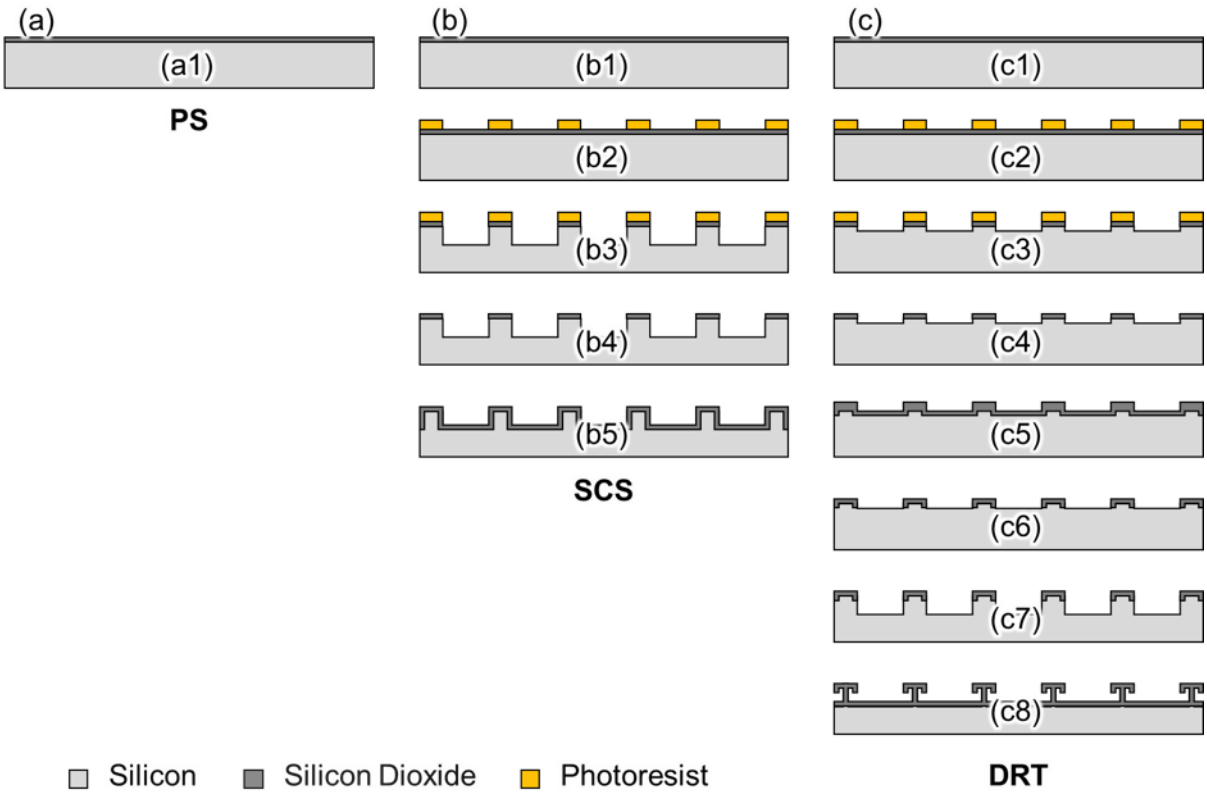

Supplementary Figure S12. The fabrication process of (a) PS, (b) SCS, and (c) DRT surface.